Geosynthetics - 7th ICG - Delmas, Gourc & Girard (eds) © 2002 Swets & Zeitlinger, Lisse ISBN 90 5809 523 1

Viscous deformation during cyclic loading of geosynthetics reinforcement

W. KONGKITKUL, D. HIRAKAWA & F. TATSUOKA, The University of Tokyo, JAPAN

ABSTRACT: Viscous deformation taking place during cyclic loading of a polymer geogrid was experimentally evaluated. Cyclic loading tests were performed at different strain rates and different load levels using different cyclic load amplitudes. Effects of creep loading on the viscous deformation during subsequent cyclic loading were evaluated. Effects of cyclic loading on the subsequent tensile load-strain behaviour were evaluated. Residual strains developed by cyclic and creep loadings were compared. Most part of residual strains taking place during the cyclic loading tests of the tested geogrid was due to viscous deformation, which was essentially a function of irreversible strain and its rate. It is shown that a non-linear three-component model that can simulate very well the elasto-visco-plastic stress-strain behaviour of soil is also relevant to the simulation of the tensile load-strain behaviour of the tested geogrid.

1 INTRODUCTION

The number of permanent geosynthetic-reinforced soil (GRS) structures is increasing due to their high cost-effectiveness and sufficiently high performance against long-term working load as well as severe seismic load. It is true however that GRS structures are relatively deformable, exhibiting more-or-less time-dependent residual deformation, when compared with reinforced concrete structures. The deformation of GRS structures could be predicted confidently only when the deformation characteristics of both geosynthetic reinforcement and backfill are well understood. To this end, the deformation characteristics of geosynthetic reinforcement during creep and cyclic loadings and their effects on the subsequent tensile load-strain behaviour have been studied extensively (e.g., Bathurst and Cai 1994; Moraci and Montanelli 1997; Ling et al. 1998). Despite the above, effects of creep and cyclic loadings have been evaluated rather separately and their possible interactions are only poorly understood.

The design tensile strength of given geosynthetic reinforcement is usually obtained by largely reducing the strength obtained from tensile rupture tests performed at a relatively high strain rate (typically 10 %/min) with a relatively large creep reduction factor. In many design codes, it is also the case with the tensile strength for seismic design. It is likely that the design method described above is linked to the isochronous concept, which says that the current tensile load is a unique function of instantaneous strain and elapsed time since the start of loading. Suppose that geosynthetic reinforcement with a load-strain state at point *X* in Fig. 1, after a long-term creep loading or stress relaxation, is subjected to seismic load. According to the isochronous concept, the tensile load cannot become greater than values along the isochronous curve $t = t_5$ (curve *XA*). That is, creep is deemed as the degradation process. The actual behaviour after loading is restarted from point *X* tends to rejoin the original curve (bound for point *B*), resuming the original strength (e.g., Voskamp et al. 2001; Zornberg and Kavanjian 2001). Hirakawa et al. (2002) showed that the rate-dependent tensile load-strain behaviour of geosynthetic reinforcement, as observed in monotonic loading tests at different strain rates as well as creep loading and stress relaxation tests, is controlled by instantaneous irreversible strain, its rate and loading history (not by elapsed time). It is very likely therefore that the conventional method, linked to the isochronous concept, could be highly conservative when obtaining the design tensile strength against seismic load.

In view of the above, a series of unconventional tensile loading tests were performed on a typical geosynthetic reinforcement to evaluate the viscous property and its effects on the tensile load-strain behaviour during cyclic loading. Part of the test results was simulated by a non-linear three-component model that was originally developed for geomaterials (soils and rocks) (Di Benedetto et al. 2002; Tatsuoka et al. 2002).

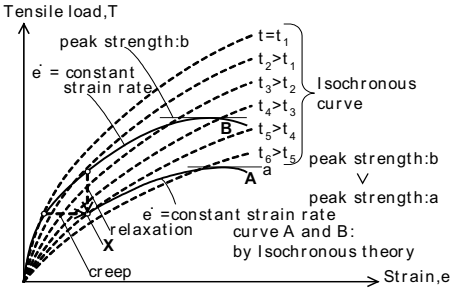

Figure 1. Tensile load-strain relationship according to the isochronous concept and actual behavior (Hirakawa et al. 2002).

2 TEST MATERIALS AND TEST PROCEDURES

A geogrid made of VECTRAN fiber was used (Table 1). Each specimen had a total initial length of 900 mm with an initial unconfined length of 240 mm and an initial gauge length of 50 mm for local axial strain measurements by using a pair of laser displacement transducers. Both ends of specimen were gripped with a pair of roller clamps, each consisting of a steel cylinder, around which the specimen is wrapped, and a small-diameter steel bar to fix the specimen end into a groove in the cylinder. In all the tests, tensile rupture took place in the central un-gripped part. An automated displacement-control loading apparatus was used, which is of precision gear type with practically no backlash when the loading direction is reversed. The tests were performed at 23±2 °C in a temperature-controlled room.

Table 1. The physical and index properties of geogrid used in this study.

Name	Super G grid (S-6000)
Fiber material	VECTRAN
dtex	8800 x 10020
Coating material	Polyvinyl chloride resin
V_{max} [1)] (kN/m)	86.2 1 strand, 50%/min
V_{max} [2)] (kN/m)	66.6 20 cm, 1%/min

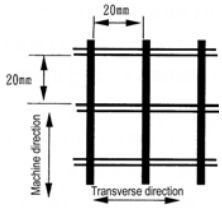

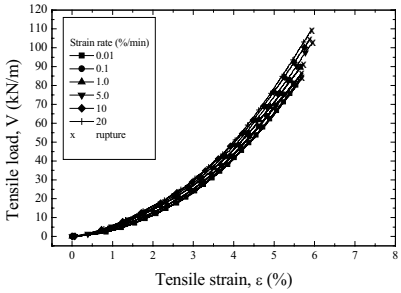

Figure 2. Tensile load-strain relationships from continuous ML tests.

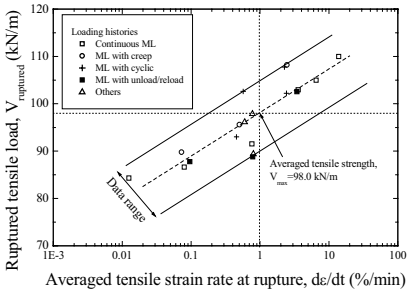

Figure 3. Tensile rupture strength versus strain rate at rupture.

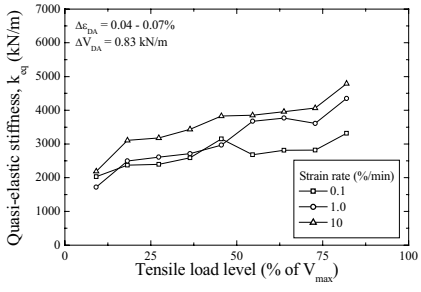

Figure 4. Quasi-elastic stiffness at different load levels and strain rates.

3 TEST RESULTS AND DISCUSSIONS

3.1 *Continuous monotonic loading tests*

Continuous monotonic loading (ML) tests were performed at constant strain rates in a range of 0.01 - 20 %/min (Fig. 2). It may be seen that the overall stiffness increased with the strain rate. Fig. 3 shows a summary of the tensile strengths from these tests and those having more complicated loading histories (explained later), plotted against the strain rate at rupture. It may be seen that the tensile strength is a rather unique function of the strain rate at rupture while nearly the same for different loading histories with different total elapsed times until rupture. These test results indicate the significance of viscous property in the behaviour of the tested geogrid, while showing that the isochronous concept is not relevant.

The peak-to-peak secant stiffness k_{eq} of the geogrid was evaluated by applying small unload/reload cycles with a double amplitude cyclic load of 0.83 kN/m, developing a double amplitude-tensile strain of 0.04~0.07 %, during otherwise ML at a constant strain rate (Fig. 4). It may be seen that the k_{eq} value increased slightly with the increase in the tensile load level. The k_{eq} value should be called the quasi-elastic stiffness as it is slightly dependent of strain rate. The average value of these k_{eq} values was used when simulating the test results.

3.2 *Creep loading tests*

Creep loading tests, each lasting for one hour, were performed at 23.3, 46.7 and 70.0 % of the averaged tensile strength at strain rate of 1%/min (98.0 kN/m) during otherwise ML at constant strain rates, 0.1, 1.0 and 5.0 %/min (Fig. 5). Subsequently ML was restarted at the respective original strain rate. Fig. 6 shows a summary of creep strains for a period of one hour plotted against creep load. Fig. 7 shows the time histories of creep strain. The simulated relations shown in Figs. 5, 6 and 7 will be explained later. The following trends of behavior may be seen from these figures.

1) Upon the restart of ML following the respective creep loading stage, the geogrid shows very high stiffness, close to the elastic value. Subsequently the tensile load-strain curve tends to rejoin the respective original ML curve. The tensile strengths from these tests including creep loading stages (denoted as "ML with creep" in Fig. 3) are essentially the same as those from the continuous ML tests at the same strain rate, showing that creep is not a degradation phenomenon.
2) The creep strain for a given period decreases with the increase in the tensile load level. This trend of behaviour is due to an increase in the tangent stiffness with the load level.
3) The creep strain for a given period decreases with the decrease in the initial creep strain rate. This trend of behaviour is due to the intrinsic viscous property of the geogrid.

The trends of behaviour 2) and 3) can be simulated by a non-linear three-component model (as shown later). The viscous property described above affects significantly the strain development during cyclic loading as shown below.

3.3 *Cyclic loading tests*

Cyclic loading tests were performed at several load levels during otherwise ML at constant strain rates, 1.0 and 5.0 %/min (Fig. 8). The strain rate during cyclic loading was the same as the one during respective ML. The peak load during the respective cyclic loading test was the same as the corresponding creep load level presented in Fig. 5. The double amplitude cyclic load was 10 and 20 kN/m. After the number of loading cycle reached 100, ML was restarted at the respective original strain rate. Fig. 9 shows a summary of the residual strains that developed during the first ten minutes in the cyclic loading tests (Fig. 8) and the creep loading tests (Fig. 7). The following trends of behaviour can be

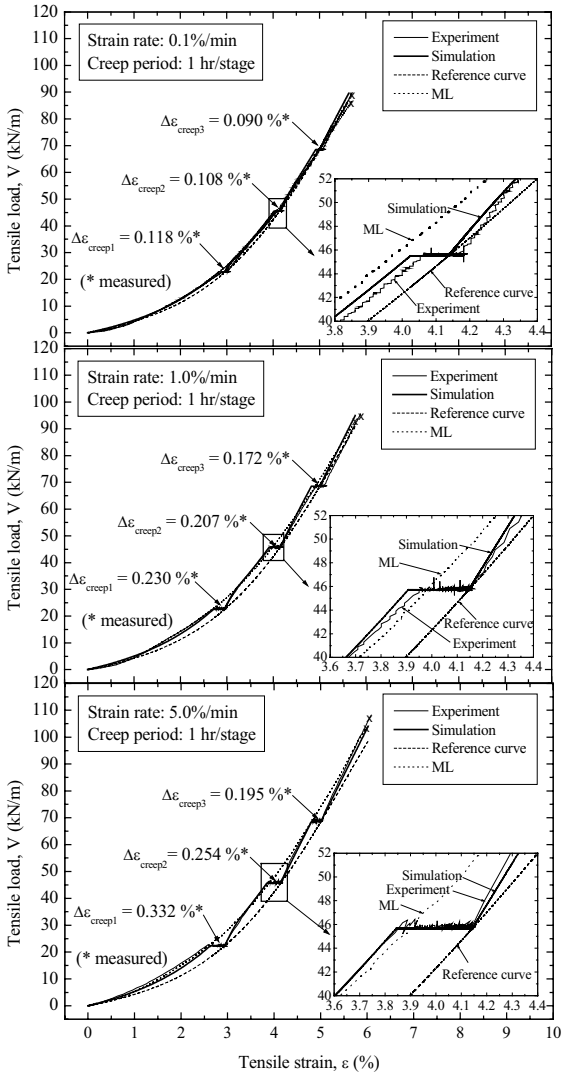

Figure 5. Measured and simulated tensile load-strain relationships from ML tests including creep loading tests.

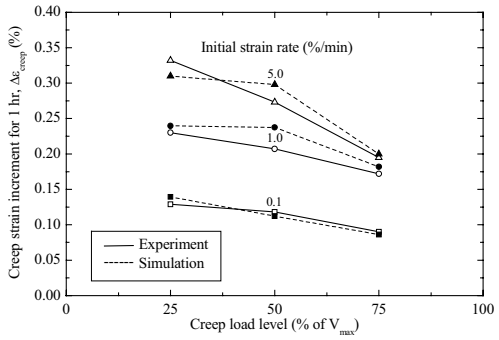

Figure 6. Measured and simulated creep strain for 1 hr versus load level for different initial creep strain rates.

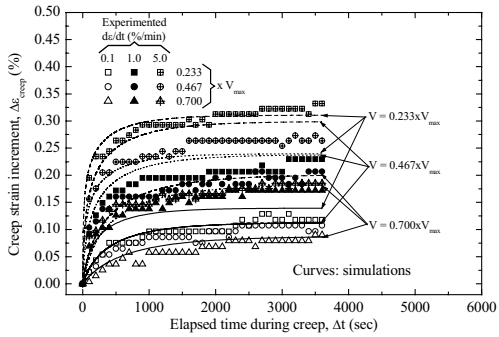

Figure 7. Measured and simulated time histories of creep strain for different load levels and initial creep strain rates.

seen from Figs. 8 and 9:

1) Similar to the post-creep behaviour (Fig. 5), the stiffness upon the restart of ML is very high and subsequently the behaviour tends to rejoin the respective original ML one. The tensile strengths from these tests (denoted as "ML with cyclic" in Fig. 3) are essentially the same as those from continuous ML tests, suggesting that cyclic loading is not a degradation phenomenon, similarly to creep loading.
2) The residual strain decreased with the increase in the peak load during cyclic loading and also with the decrease in the strain rate, similarly to the creep behaviour (Fig. 6). These trends of behaviour could be explained as the effects of viscous property, not by the effects of cyclic loading.
3) The residual strain decreases with the increase in the cyclic load amplitude. This trend of behaviour is consistent with the fact that the for the same peak load and for the same loading duration, the residual strain in the cyclic loading tests is generally similar to or smaller than the one in the creep loading tests (i.e., zero load amplitude cyclic loading tests) (Fig. 9). This trend of behaviour could also be explained as the effects of viscous property, not by the effects of cyclic loading.

To confirm the trend 3), the geogrid was subjected to ML at a strain rate of 1 %/min until the tensile load became 66.67 kN/m and then creep loading was performed for 10 min (Fig. 10). Subsequently, a sequence of 100 cycles of a double amplitude cyclic load of 5 kN/m and creep loading for 10 minutes was applied. This sequence was repeated with increasing the cyclic load amplitude. Finally, the specimen was subjected to ML at the original strain rate towards the ultimate rupture. Fig. 10c shows the time histories of residual strain at the first creep stage and the first cyclic loading stage with a cyclic load amplitude of 5 kN/m, as marked by the letters '*a*' to '*b*' and '*b*' to '*c*' in Fig. 10b. The following trends of behaviour may be seen from Fig. 10:

1) The residual strain that developed during the first creep stage is particularly large. The residual strain developed during the first cyclic loading stage is much smaller while those at the subsequent creep and cyclic loading stages are very small.

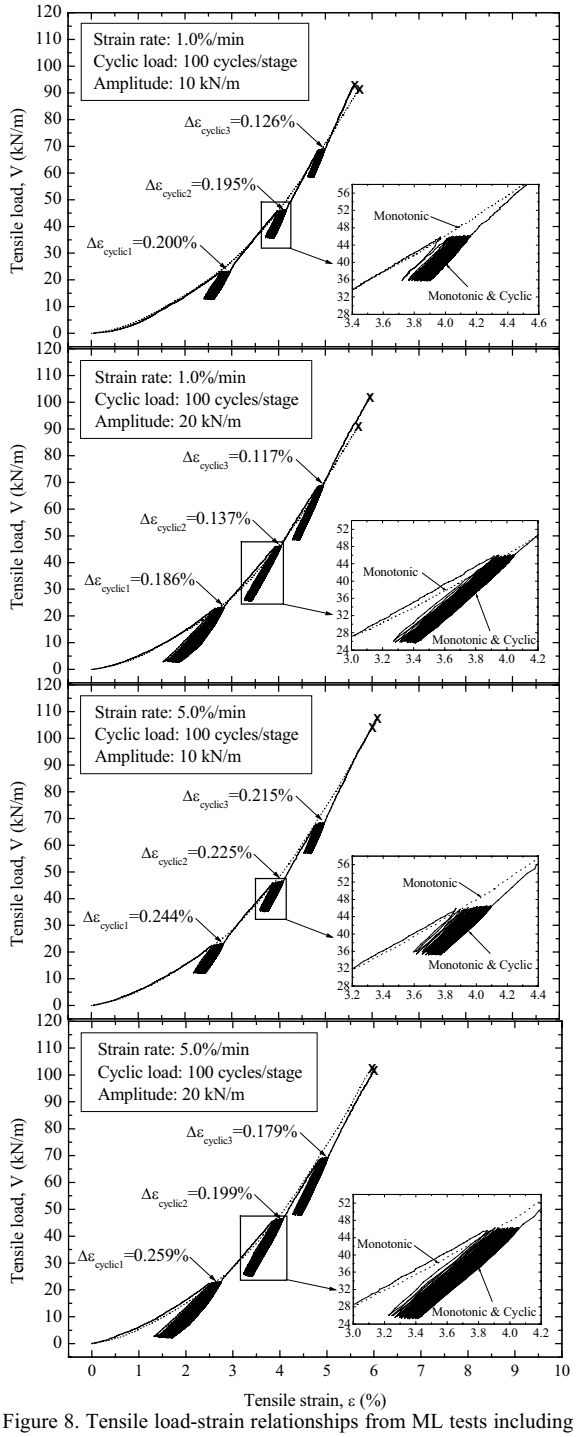

Figure 8. Tensile load-strain relationships from ML tests including cyclic loading tests at different strain rates.

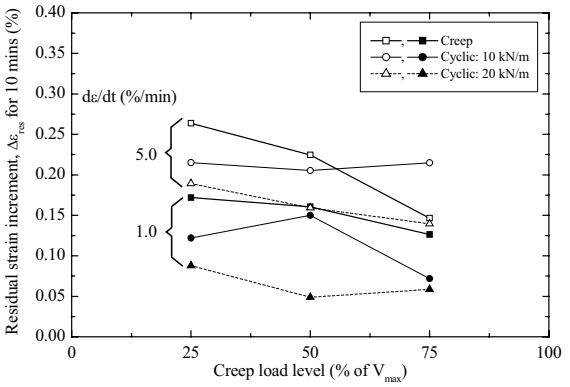

Figure 9. Residual strains versus load level from cyclic and creep loading tests for different strain rates.

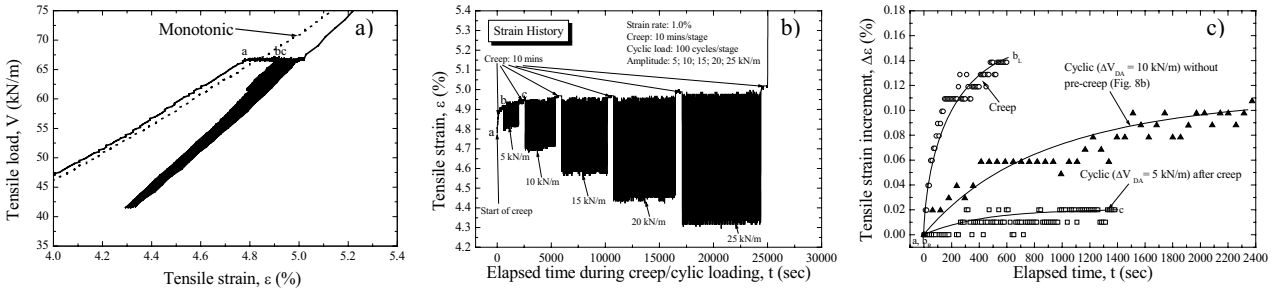

Figure 10. a) Tensile load-strain relationships from ML tests including creep/cyclic loading tests; b) tensile strain history and c) time histories of residual strain from creep and cyclic

2) The residual strain developed during the first cyclic loading stage is smaller than the value by similar cyclic loading without pre-creep loading (from Fig. 8b) (see Fig. 10c).

These test results show that the effects of loading history, including creep loading, on residual strains that develop at subsequent cyclic loading stages could be significant, because most of the residual strain developing during cyclic loading is viscous one. This factor should be accounted for when evaluating the residual deformation during cyclic loading.

4 SIMULATION OF CREEP TEST RESULTS

4.1 *Three-component model*

According to the non-linear three-component model (referred to Fig. 6 in Tatsuoka et al. 2002), the tensile load-strain (V~ε) behaviour of geosynthetic reinforcement can be obtained as follows:

$$V = V^f(\varepsilon^{ir}) \cdot \{1 + g_v(\dot{\varepsilon}^{ir})\} \quad (1)$$

where $V^f(\varepsilon^{ir})$ is the inviscid load that is a unique function of instantaneous irreversible strain ε^{ir}, which is equal to $\varepsilon - \varepsilon^e$; and $g_v(\dot{\varepsilon}^{ir})$ is the viscosity function, given as:

$$g_v(\dot{\varepsilon}^{ir}) = \alpha \cdot \left[1 - \exp\left\{1 - \left(\dot{\varepsilon}^{ir}/\dot{\varepsilon}_r^{ir} + 1\right)^m\right\}\right] \quad (2)$$

where $\dot{\varepsilon}^{ir}$ is the irreversible strain rate and α, m and $\dot{\varepsilon}_r^{ir}$ are the material constants. The elastic strain rates are obtained as $\dot{\varepsilon}^e = \dot{V}/k_{eq}(V)$ ($k_{eq}(V)$= 3,500 kN/m is assumed).

Figure 5 also shows the results from the simulation of the test results. In the simulation, the time history of load was obtained for a given time history of strain by using; α = 0.44, m = 0.09 and $\dot{\varepsilon}_r^{ir}$ = 0.001 %/min. These parameters were determined by performing ML tests with many step changes in the strain rate. The V^f~ε^{ir} relationship was determined by the method of best fitting. The results of the simulation are also presented in Figs. 6 and 7. It may be seen from these figures that the proposed model can simulate rather accurately the various viscous aspects observed for a wide range of loading histories. As the same model parameters were used for all these tests, some discrepancy between the measured and simulated behaviors is due mostly to an inevitable scatter in the material properties among the different specimens. The three-component model can also simulate viscous deformation during unloading and reloading of geomaterial (Tatsuoka et al. 2001; Hayano et al. 2001) and geosynthetic reinforcement (Kongkitkul et al. 2002).

5 CONCLUSIONS

The following conclusions can be derived from the results from the present experimental and theoretical study:

1) The tensile load-strain behaviour and tensile strength of the tested geogrid during cyclic loading was rate-dependent and the residual deformation that developed during cyclic loading was essentially viscous one. So, the residual deformation developed during cyclic loading became substantially small by pre-creep loading.
2) The tensile load-strain behaviour of the tested geogrid was essentially a unique function of instantaneous irreversible strain rate. So, the stiffness upon the restart of loading after creep or cyclic loading was very high and subsequently the behaviour tended to rejoin the original one at the respective strain rate. The tensile strength was controlled uniquely by the strain rate at rupture, not affected by loading histories of creep, stress relaxation and cyclic loading applied before the rupture. That is, creep and cyclic loadings are not degradation phenomena.
3) The non-linear three-component model, originally developed for geomaterials, also relevant to the simulation of the rate-dependent tensile load-strain behaviour of the tested geogrid.
4) It is not necessary to reduce the tensile strength of geosynthetic reinforcement by using a large creep reduction factor to obtain the design strength for not only monotonic but also cyclic loading as long as the creep failure is not likely to occur for a given designed life time.

6 ACKNOWLEDGEMENT

The test material was provided by Taiyo Kogyo Co. Ltd.

7 REFERENCES

Bathurst, R.J. and Cai,Z. 1994. In-isolation cyclic load-extension behavior of two geogrid, *Geosynthetics International*, Vol.1, No.1, pp.3-17.

Di Benedetto ,H., Tatsuoka, F. and Ishihara, M. 2002. Time-dependant shear deformation characteristics of sand and their constitutive modeling, *Soils and Foundations*, 42 (2).

Hayano, K., Matsumoto, M. Tatsuoka, F. and Koseki, J. 2001. Evaluation of time-dependent deformation property of sedimantary soft rock and its consitutive modeling, *Soils and Foundations,* Vol.41, No.2, pp.21-38.

Hirakawa, D., Uchimura, T., Shibata, Y. and Tatsuoka, F. 2002. Time-dependant deformation of geosynthetics and geosynthetic-reinforced soil structures, *Proc. 7th International Conference on Geosynthetics, Nice*, Vol. 1 (to be published).

Kongkitkul, W., Hirakawa, D. and Tatsuoka, F. 2002. Viscous effects on load-deformation characteristics of geogrid during unloading and reloading and model simulation, *Proc. 37th Japan National Conf. on Geotechnical Engineering, JGS* (Osaka).

Ling, H.I., Mohri, Y., and Kawabata, T. 1998. Tensile Properties of Geogrids under Cyclic Loadings, *Journal of Geotechnical and Geoenvironmental Engineering*, ASCE, Vol. 124, No.8, pp. 782-787.

Moraci, N. and Montanelli, F. 1997. Behavior of geogrids under cyclic loads, *Proc. Geosynthetic '97 Conf.*, pp.996-976.

Tatsuoka,F., Ishihara,M., Di Benedetto,H. and Kuwano,R. 2002. Time-dependent shear deformation characteristics of geomaterials and their simulation, *Soils and Foundations*, 42 (2).

Voskamp, W., van Vliet, F. and Retzlaff, J. 2001. Residual strength of PET after more than 12 years creep loading, *Landmarks in Earth Reinforcement, Ochiai et al. (eds) © 2001 Swets & Zeitlinger*, Vol.1, pp.165-170.

Zornberg, J.G. and Kavazanjian, E.Jr. 2001. Prediction of the performance of a geogrid–reinforced slope founded on solid waste. *Soils and Foundations,* Vol.41, No.6, pp.1-6.